Published in final edited form as:
Biochem Biophys Res Commun. 2008 November 21; 376(3): 573–577. doi:10.1016/j.bbrc.2008.09.031.

Induction of Follistatin Precedes Gastric Transformation in Gastrin Deficient Mice

Weiqun Kang[1], **Milena Saqui-Salces**[1], **Yana Zavros**[1], and **Juanita L. Merchant**[1,2*]

1*Department of Internal Medicine, Cell and Developmental Biology, University of Michigan, Ann Arbor, MI USA*

2*Department of Molecular and Integrative Physiology, University of Michigan, Ann Arbor, MI USA*

Abstract

We previously showed that antral gastric tumors develop in gastrin-deficient ($Gas^{-/-}$) mice. Therefore $Gas^{-/-}$ mice were studied sequentially over 12 months to identify molecular mechanisms underlying gastric transformation. Fundic atrophy developed by 9 months in $Gas^{-/-}$ mice. Antral mucosal hyperplasia developed coincident with the focal loss of TFF1 and Muc5AC. Microarray analysis of 12 month $Gas^{-/-}$ tumors revealed an increase in follistatin, an activin/BMP antagonist. We found that elevated follistatin expression occurred in the proliferative neck zone of hyperplastic antrums, in antral tumors of $Gas^{-/-}$ mice, and also in human gastric cancers. Follistatin induced cyclin D1 and the trefoil factors TFF1 and TFF2 in a gastric cancer cell line. We concluded that antral hyperplasia in $Gas^{-/-}$ mice involves amplification of mucous cell lineages due to follistatin, suggesting its role in the development of antral gastric tumors.

Keywords

Gastrin; intestinal metaplasia; TFF1; atrophic gastritis; mucous neck cell; gastric cancer; Muc6; activins; follistatin

Introduction

Gastric cancer is the fourth most common cancer and the second most common cause of cancer-related deaths in the world [1,2]. The molecular mechanisms underlying the sequential phenotypic changes in the gastric mucosa from chronic inflammation (gastritis) to atrophy, metaplasia then eventually cancer are not well defined [3]. An increasing number of signaling pathways and regulatory molecules have been suggested to play a role in gastric transformation, e.g., TFF1 [4] Smad4, [5] Runx3 [6], STAT3 [7] [8] and Klf4 [9]. Several of these pathways implicate epithelial-mesenchymal crosstalk with TGFβ family members, e.g., activins, Smad4, Runx3. Gordon and coworkers showed that high levels of activin A in the α-inhibin null mouse induces expansion of the mucous neck and surface pit lineages, suggesting that activin-dependent signaling affects the proliferative activity and differentiation of gastric stem cells [10]. Follistatin is an antagonist of the activin and BMP ligands. Moreover, an increase in

Correspondence: Juanita L. Merchant, M.D., Ph.D., 109 Zina Pitcher Place, BSRB 2051, Ann Arbor, MI 48109-2200, E-mail: merchanj@umich.edu, Phone: 734-647-2944.

follistatins correlates with an increase in proliferation and counteracts activin-induced apoptosis [11]. Prior studies have suggested that increased follistatin levels partially block the wasting syndrome observed under activin overexpression [12]. However, little is known regarding the role of follistatin in gastric neoplasia.

Reports from tumor registries and more recent histological mapping studies show that approximately 50% of intestinal-type gastric cancers are located in the antrum, 38% are in the corpus and 12% are located at the incisura [13]. Therefore, corpus atrophy appears to correlate with tumors developing in the distal rather than the acid-secreting portion of the stomach. This observation raises the possibility that the linkage is not arbitrary but rather may reveal mechanisms that influence cancer pathogenesis. We previously demonstrated that $Gas^{-/-}$ develop antral tumors by 12 months of age and exhibit reduced TFF1 expression and elevated phosphorylated STAT3 expression [14]. Therefore, we used a microarray analysis of $Gas^{-/-}$ tumors to identify molecules involved in tumor pathogenesis, and based on the role of the activin pathway in gastric epithelial lineages differentiation demonstrated in transgenic mice [10], we found that follistatin was significantly uprregulated, supporting the importance of this pathway in tumorigenesis.

Materials and Methods

Human samples

Human normal and tumor protein extracts and tissue sections without patient identifiers were obtained from Bio Chain Institute, Inc. (Hayward, CA).

Animals

Gastrin deficient ($Gas^{-/-}$) and strain-matched wild-type (WT) control mice were maintained on a mixed 129/Sv-C57/BL6 background [15]. The animals were housed in microisolator, solid-bottom polycarbonate cages in non-barrier mouse rooms. The study was performed with the approval of the University of Michigan Animal Care and Use Committee, which maintains an American Association for the Assessment and Accreditation of Laboratory Animal Care facility.

Immunohistochemical Analysis

A longitudinal section of the mouse stomach (spanning both fundus and antrum) was fixed in 4% paraformaldehyde in PBS, and paraffin-embedded. Four μm sections were subsequently prepared. Antigen retrieval was performed for all antibodies by microwaving in 10 mM citrate buffer (pH 6.0) for 10 min. Sections were incubated with the primary antibodies at 4°C overnight; 1:500 dilution of biotin-conjugated secondary antibodies was then added for 30 min at 25°C and visualized with avidin-biotin complexes (Vectastain Elite ABC) and diaminobenzidine (DAB) (Vector Laboratories). For immunofluorescence, Alexa labeled secondary antibodies (Invitrogen) at 1:500 dilution were incubated for 30 min at 25°C, before staining with 4',6-diamidino-2-phenylindole (DAPI).

The primary antibodies used were: rabbit anti-TFF2 (1:1000 dilution, a gift from Dr. Andy Giraud, University of Melbourne, Australia), polyclonal goat anti-TFF1 (pS2) (1:100 dilution, Santa Cruz); Muc5AC (1:50 dilution, Santa Cruz), mouse monoclonal anti-Muc6 (1:200 dilution, Novocastra), goat polyclonal anti-Ki67 (1:500 dilution, Pharmingen), anti-β subunit of the H^+, K^+-ATPase (1:1000 dilution, BCL), plant lectin *Griffonia Simplicifolia* II (GSII), [16] at a 1:1000 dilution (Vector Laboratories), and rabbit polyclonal anti-follistatin (1:50 dilution, Santa Cruz).

Immunoblots

Stomachs removed from WT and $Gas^{-/-}$ mice were opened along the greater curve then cut along the incisura to separate the antrum from the corpus. Protein was extracted from antral and fundic tissues, using T-per lysis buffer (Pierce) supplemented with protease inhibitors (Roche). After centrifuging the lysate for 10 min at 10,000 × g, 50 μg of protein extract were resolved using 4–20% gradient SDS-PAGE and then transferred onto nitrocellulose membranes. Immunoblot analysis was performed at 4°C overnight, using anti-Muc5AC and mouse monoclonal anti-N-myc (Novus). The signals were visualized with an ECL detection system (Amersham). The membrane was stripped and re-blotted against GAPDH to normalize the input.

NCI-N87, AGS, and MKN-45 cells were grown to confluence and serum starved for 24 h. The cells were lysed using RIPA buffer (Sigma) and proteins were resolved on SDS-PAGE gels and analyzed for follistatin (Santa Cruz), as described above. Additionally, whole cell extracts of follistatin treated NCI-N87 cells were blotted for cyclin D1 (rabbit polyclonal, Santa Cruz), TFF1 and TFF2 (both goat polyclonal antibodies, Santa Cruz).

Quantitative RT-PCR

The PCR primer sequences used to amplify Muc6 and GAPDH cDNA were as previously described [17]. The fluorogenic probe (100 nM, Research Genetics Inc., Huntsville, Al, USA) was used for all quantitative PCR analysis. The reactions were carried out in a total volume of 25 μl in triplicate wells in a BioRad iCycler (Hercules, CA). The fold change for each $G^{-/-}$ mouse was calculated as suggested by Livak and Schmittgen [18]: 2ΔΔCT=fold change, and ΔΔCT=(CT, Target, -CT,GAPDH)G−/− (CT, Target,-CT,GAPDH)WT, where CT=threshold cycle and (CT,Target,-CT,GAPDH) WT=mean value for seven WT mice.

Primary cell preparation and Flow cytometry

Epithelial cells were isolated from the gastric mucosa from individual mice. Briefly, the corpus was separated from the antrum and dissected into 2-mm size pieces. The pieces were incubated in 20 ml of Hank's balanced salt solution containing 5% bovine serum albumin, 1 mM dithiothreitol, and 1mM EDTA for 1 h with vigorous shaking at 37°C to release the epithelial cell population. This first cell suspension was filtered (50 μm Filcon filter; Dako), collected, and washed twice with RPMI1640 medium with 5% fetal calf serum. The stripped mucosa was then subjected to enzymatic digestion in 20 ml of RPMI medium with 1 mg/ml dispase II (Roche) for two 60 min incubations at 37°C with vigorous shaking. The total number of cells isolated from each WT corpus was $1.5\sim2 \times 10^6$, and $0.9 \sim 1.2 \times 10^6$ from each 12 mo old $Gas^{-/-}$ stomach. Mucous neck cells were detected with the FITC-conjugated lectin GSII, after permeabilization. Labeled cells were analyzed using FACScan (Beckman Dickson). Data were analyzed using CellQuest Software (Becton Dickinson). The number of GSII positive mucous neck cells per corpus was calculated as follows: (Total cell number/corpus) × (%GSII positive cells).

Microarray Analysis

Total RNA was extracted from three antrums from WT mice and $Gas^{-/-}$ mice, all 12 mo for generation of cDNA and probe generation by the University of Michigan Microarray Core. The quantity and quality of the RNA was verified on an Agilent 2100 BioAnalyzer. The mouse Affymetrix Gene Chip was probed after fluorescent labeling.

Follistatin treatment

NCI-N87 (ATCC) and AGS (ATCC) cells were grown to confluence in RPMI-1640 media supplemented with 10% FBS and 1% streptomycin. Cell cultures were serum starved for 24 h

and then treated with 0.5 μg/ml human recombinant-follistatin (R&D Systems) in serum free media for 24 h. Whole cell extracts were obtained, resolved on SDS-PAGE gels, transferred onto nitrocellulose membranes then immunoblotted as described above.

Statistical Analysis

The mean ± the standard error of the mean (SEM) was calculated and compared to controls using the unpaired *t*-test from the commercially available software Prism 3 (GraphPad Software, San Diego, CA, USA). A P-value of <0.05 was considered significant.

Results

Gastric atrophy and mucous cell hyperplasia develops in 9 month old $Gas^{-/-}$ mice

We have previously shown that parietal cell atrophy and distal gastric tumors occur in 12 month old $Gas^{-/-}$ mice [14]. Yet, early molecular changes correlating with the parietal cell loss, i.e., corpus atrophy, are not clearly described. Therefore, we examined histologic markers defining the glandular stomach prior to 12 months in $Gas^{-/-}$ mice. Immunodetection of the H^+K^+-ATPase beta subunit demonstrated a significant reduction in the number of parietal cells even as early as 9 months (Fig. 1A–C). There was an increase in the surface mucous compartment documented by immunostaining for Muc5AC (Fig. 1D–F). Enumeration of Ki-67-positive cells in the $Gas^{-/-}$ corpus compared to WT mice revealed a 2.5-fold increase (Fig. 1G–I). The decrease in parietal cells demonstrated by reduced H^+,K^+-ATPase coincided with an increase in mucous neck cells demonstrated by increased GSII and Muc6 expression (Fig. 1J, I). Indeed, quantification of the total number of neck cells in the corpuses of 12 month $Gas^{-/-}$ mice by flow cytometry confirmed that there was an ~18% increase in the $Gas^{-/-}$ mice compared to WT mice (data not shown). Collectively, these data demonstrated hyperplasia of both the surface mucous and neck cell compartments at the expense of parietal cells.

Antral hyperplasia in $Gas^{-/-}$ mice

At the same time that parietal cell atrophy and expansion of the mucous cell compartments was observed, the antrum became hyperplastic. In the antrum, the proliferating cells expressing Ki-67 correlated with mucosal elongation (Suppl. Fig. 1A and B). By 12 months, the Ki-67 staining cells overlapped with the GSII-positive pyloric gland cells that were also TFF2 positive (data not shown) demonstrating that the antral mucous neck cell lineage was also expanding (Suppl. Fig. 1C and D).

The antral surface pit cell lineage was examined using TFF1 immunostaining. TFF1 was detected above the hyperplastic mucous neck cell compartment in WT and 9 month $Gas^{-/-}$ mice (Suppl. Fig. 1E and F). We also observed a distinct cell boundary separating normal TFF1-positive areas from the neighboring hyperplastic cell population that exhibited reduced TFF1, Muc5AC and PAS staining (Suppl. Fig. 1G–I) in $Gas^{-/-}$ antrums by 12 months. These results suggested an increase in the neck cell lineage, and reduced surface mucous cell differentiation at the transition from hyperplastic to dysplastic antrums.

Follistatin expression increased in gastric tumors

To identify the molecular pathways that were modulated in the gastric antrum during transformation, we performed a microarray analysis on three tumors from 12 month old $Gas^{-/-}$ mice and compared the results to age-matched controls. Table 1 shows relevant genes that were up- or down-regulated >2 fold in the antral tumors. Gastrin and H^+K^+-ATPase mRNA levels were >20-fold depressed in the microarray, confirming that the samples used for the analysis were gastrin-deficient and had little or no corpus tissue, which would have been H^+K^+-ATPase positive. A number of pathways were represented in the up-regulated set of

genes including tissue metalloproteases, IL-1β and related molecules, EGF receptor ligands, e.g., amphiregullin, epiregulin; TGFβ family members, Inhibin bA and follistatin; and the Notch ligand jagged. Interestingly, several of the genes regulated in this $Gas^{-/-}$ mouse model, e.g., metalloproteases and amphiregulin, are also modulated in the *H. felis*-infected INS-GAS model [19]. To our knowledge, this is the first report of TGFβ family members inhibin bA and follistatin overexpression in gastric tumors.

The expression of follistatin was dramatically increased in the antral mucosa of 9 month $Gas^{-/-}$ compared to age-matched WT mice (Suppl. Fig. 2A–C) and correlated with an expansion of the mucous neck cells (GSII staining in Suppl. Fig. 2B). Follistatin-expressing cells overlapped with the proliferation marker Ki-67 in both the hyperplastic antrum (Suppl. Fig. 2E), and $Gas^{-/-}$ tumor (Suppl. Fig. 2F).

Follistatin is expressed in normal human antrum, and its expression is significantly increased in tubular adenocarcinoma (Fig. 2A,B), and signet ring carcinoma (Fig. 2C), suggesting a participation of this protein in the development of human gastric cancer. To determine whether elevated levels of follistatin induced proliferation, three human gastric cell lines were screened for follistatin expression. Interestingly, only the mucopeptic cell line NCI-N87 expressed follistatin. Treatment of this cell line with follistatin for 24h induced the proliferation marker cyclin D1 and the mucous lineage specific proteins TFF1 and 2 suggesting that follistatin promotes mucous cell proliferation and differentiation. The less differentiated AGS cells were not responsive to follistatin treatment (data not shown), suggesting that effect of follistatin is cell type dependent.

Discussion

The spatial and cellular aspects of tumor development observed in $Gas^{-/-}$ mice [14] is very similar to that of the TFF1 knockout mouse [4] and the $gp130^{757F/F}$ mouse [8]. In this study, further analysis demonstrated that well-defined regional loss of surface mucous cells (TFF1 expression) occurred in the hyperplastic antrum. Consistent with the TFF1-deficient mice model, there were apparently lower levels of TFF1 than TFF2 in hiperplastic $Gas^{-/-}$ antrums (data not shown). This result suggested that more of the hyperplastic cells were phenotypically of the mucous neck cell lineage.

Follistatin is a single-chain glycoprotein that was first isolated from ovarian follicular fluids, and inhibits follicle stimulating hormone (FSH) secretion in the pituitary [20], but it also binds activins preventing receptor activation. Activins have been shown to exert regulatory effects on growth, proliferation and differentiation in different cell types [11,21,22]. In addition to activins, follistatin also binds bone morphogenetic proteins (BMP), including BMP-2,-4,-7 and 11 [23], in a cell specific way.

Activin receptor activation is necessary for foregut development, and it has been reported that activin A signaling promotes differentiation of pancreatic into intestinal tissue [24]. In 12 month $Gas^{-/-}$ mice, we observed overexpression of follistatin, but not activin. Previously, Becker et al. reported low levels of activin A expression in normal gastric samples, but a significant increase in activin A within the tissue surrounding experimentally-induced ulcers in rats [25]. Follistatin expression is induced by several signal transduction pathways including, EGF, PKA, PKC and steroid hormones [20] and strongly induced by activin A through Smad proteins [22]. Thus, the elevated levels of follistatin in the $Gas^{-/-}$ mouse antrums and human tumors, in absence of activin A, might represent induction by EGF or PKA, PKC. Interestingly, activin receptor II gene expression in $Gas^{-/-}$ mice was down-regulated (1.53-fold), suggesting muted activin signaling in the hyperplastic and dysplastic $Gas^{-/-}$ mice.

Follistatin expression was observed in areas of highly proliferative mucous cells in $Gas^{-/-}$ mice antrums. NCI-N87 is a mucous producing-cell line of well-differentiated gastric tumor origin, while AGS and MKN cells are non-mucous, poorly differentiated gastric adenocarcinoma cell lines. Only NCI-N87 cells express and response to follistatin. To our knowledge, this is the first report of follistatin activity in absence of activins. The pathways involved in the differential cell response are currently under study.

In summary, the hyperplasia and dysplasia in the antrums of $Gas^{-/-}$ mice is comprised mainly of mucous cells and includes both neck and surface cell lineages. The presence of elevated follistatin levels in mouse antral tumors and human gastric cancer suggests that neutralizing the TGF-β signaling pathway plays a role in mucous cell proliferation in the stomach.

Supplementary Material

Refer to Web version on PubMed Central for supplementary material.

Acknowledgements

This work was supported in part by Public Health Service Grant R01-DK61410 to J.L.M. and the Michigan Gastrointestinal Peptide Research Center P30-DK34933.

References

1. Pisani P, Parkin DM, Bray F, Ferlay J. Estimates of the worldwide mortality from 25 cancers in 1990. Int J Cancer 1999;83:18–29. [PubMed: 10449602]
2. Parkin DM, Bray F, Ferlay J, Pisani P. Estimating the world cancer burden: Globocan 2000. Int J Cancer 2001;94:153–156. [PubMed: 11668491]
3. Correa P, Haenszel W, Cuello C, Tannenbaum S, Archer M. A model for gastric cancer epidemiology. Lancet 1975;2:58–60. [PubMed: 49653]
4. Lefebvre O, Chenard MP, Masson R, Linares J, Dierich A, LeMeur M, Wendling C, Tomasetto C, Chambon P, Rio MC. Gastric mucosa abnormalities and tumorigenesis in mice lacking the pS2 trefoil protein. Science 1996;274:259–262. [PubMed: 8824193]
5. Xu X, Brodie SG, Yang X, Im YH, Parks WT, Chen L, Zhou YX, Weinstein M, Kim SJ, Deng CX. Haploid loss of the tumor suppressor Smad4/Dpc4 initiates gastric polyposis and cancer in mice. Oncogene 2000;19:1868–1874. [PubMed: 10773876]
6. Li QL, Ito K, Sakakura C, Fukamachi H, Inoue K, Chi XZ, Lee KY, Nomura S, Lee CW, Han SB, Kim HM, Kim WJ, Yamamoto H, Yamashita N, Yano T, Ikeda T, Itohara S, Inazawa J, Abe T, Hagiwara A, Yamagishi H, Ooe A, Kaneda A, Sugimura T, Ushijima T, Bae SC, Ito Y. Causal relationship between the loss of RUNX3 expression and gastric cancer. Cell 2002;109:113–124. [PubMed: 11955451]
7. Tebbutt NC, Giraud AS, Inglese M, Jenkins B, Waring P, Clay FJ, Malki S, Alderman BM, Grail D, Hollande F, Heath JK, Ernst M. Reciprocal regulation of gastrointestinal homeostasis by SHP2 and STAT-mediated trefoil gene activation in gp130 mutant mice. Nat Med 2002;8:1089–1097. [PubMed: 12219085]
8. Judd LM, Alderman BM, Howlett M, Shulkes A, Dow C, Moverley J, Grail D, Jenkins BJ, Ernst M, Giraud AS. Gastric cancer development in mice lacking the SHP2 binding site on the IL-6 family co-receptor gp130. Gastroenterology 2004;126:196–207. [PubMed: 14699500]
9. Katz JP, Perreault N, Goldstein BG, Actman L, McNally SR, Silberg DG, Furth EE, Kaestner KH. Loss of Klf4 in mice causes altered proliferation and differentiation and precancerous changes in the adult stomach. Gastroenterology 2005;128:935–945. [PubMed: 15825076]
10. Li Q, Karam SM, Coerver KA, Matzuk MM, Gordon JI. Stimulation of activin receptor II signaling pathways inhibits differentiation of multiple gastric epithelial lineages. Mol Endocrinol 1998;12:181–192. [PubMed: 9482661]

11. Stove C, Vanrobaeys F, Devreese B, Van Beeumen J, Mareel M, Bracke M. Melanoma cells secrete follistatin, an antagonist of activin-mediated growth inhibition. Oncogene 2004;23:5330–5339. [PubMed: 15064726]
12. Cipriano SC, Chen L, Kumar TR, Matzuk MM. Follistatin is a modulator of gonadal tumor progression and the activin-induced wasting syndrome in inhibin-deficient mice. Endocrinology 2000;141:2319–2327. [PubMed: 10875231]
13. El-Zimaity HM, Ota H, Graham DY, Akamatsu T, Katsuyama T. Patterns of gastric atrophy in intestinal type gastric carcinoma. Cancer 2002;94:1428–1436. [PubMed: 11920498]
14. Zavros Y, Eaton KA, Kang W, Rathinavelu S, Katukuri V, Kao JY, Samuelson LC, Merchant JL. Chronic gastritis in the hypochlorhydric gastrin-deficient mouse progresses to adenocarcinoma. Oncogene 2005;24:2354–2366. [PubMed: 15735748]
15. Friis-Hansen L, Sundler F, Li Y, Gillespie PJ, Saunders TL, Greenson JK, Owyang C, Rehfeld JF, Samuelson LC. Impaired gastric acid secretion in gastrin-deficient mice. Am J Physiol 1998;274:G561–G568. [PubMed: 9530158]
16. Lyer PN, Wilkinson KD, Goldstein LJ. An -N-acetyl-D-glycosamine binding lectin from Bandeiraea simplicifolia seeds. Arch Biochem Biophys 1976;177:330–333. [PubMed: 999292]
17. Kang W, Rathinavelu S, Samuelson LC, Merchant JL. Interferon gamma induction of gastric mucous neck cell hypertrophy. Lab Invest. 2005
18. Livak KJ, Schmittgen TD. Analysis of relative gene expression data using real-time quantitative PCR and the 2(-Delta Delta C(T)) Method. Methods 2001;25:402–408. [PubMed: 11846609]
19. Takaishi S, Wang TC. Gene expression profiling in a mouse model of Helicobacter-induced gastric cancer. Cancer Sci 2007;98:284–293. [PubMed: 17270017]
20. Michel U, Farnworth P. Follistatin steady state messenger ribonucleic acid levels in confluent cultures of a rat renal mesangial cell line are regulated by multiple factors. Endocrinology 1992;130:3684–3693. [PubMed: 1375907]
21. van Eyll JM, Pierreux CE, Lemaigre FP, Rousseau GG. Shh-dependent differentiation of intestinal tissue from embryonic pancreas by activin A. J Cell Sci 2004;117:2077–2086. [PubMed: 15054113]
22. Bartholin L, Maguer-Satta V, Hayette S, Martel S, Gadoux M, Corbo L, Magaud JP, Rimokh R. Transcription activation of FLRG and follistatin by activin A, through Smad proteins, participates in a negative feedback loop to modulate activin A function. Oncogene 2002;21:2227–2235. [PubMed: 11948405]
23. Iemura S, Yamamoto TS, Takagi C, Uchiyama H, Natsume T, Shimasaki S, Sugino H, Ueno N. Direct binding of follistatin to a complex of bone-morphogenetic protein and its receptor inhibits ventral and epidermal cell fates in early Xenopus embryo. Proc Natl Acad Sci U S A 1998;95:9337–9342. [PubMed: 9689081]
24. Kim SK, Hebrok M, Li E, Oh SP, Schrewe H, Harmon EB, Lee JS, Melton DA. Activin receptor patterning of foregut organogenesis. Genes Dev 2000;14:1866–1871. [PubMed: 10921901]
25. Becker JC, Hertel M, Markmann A, Shahin M, Werner S, Domschke W, Pohle T. Dynamics and localization of activin A expression in rat gastric ulcers. Scand J Gastroenterol 2003;38:260–267. [PubMed: 12737440]

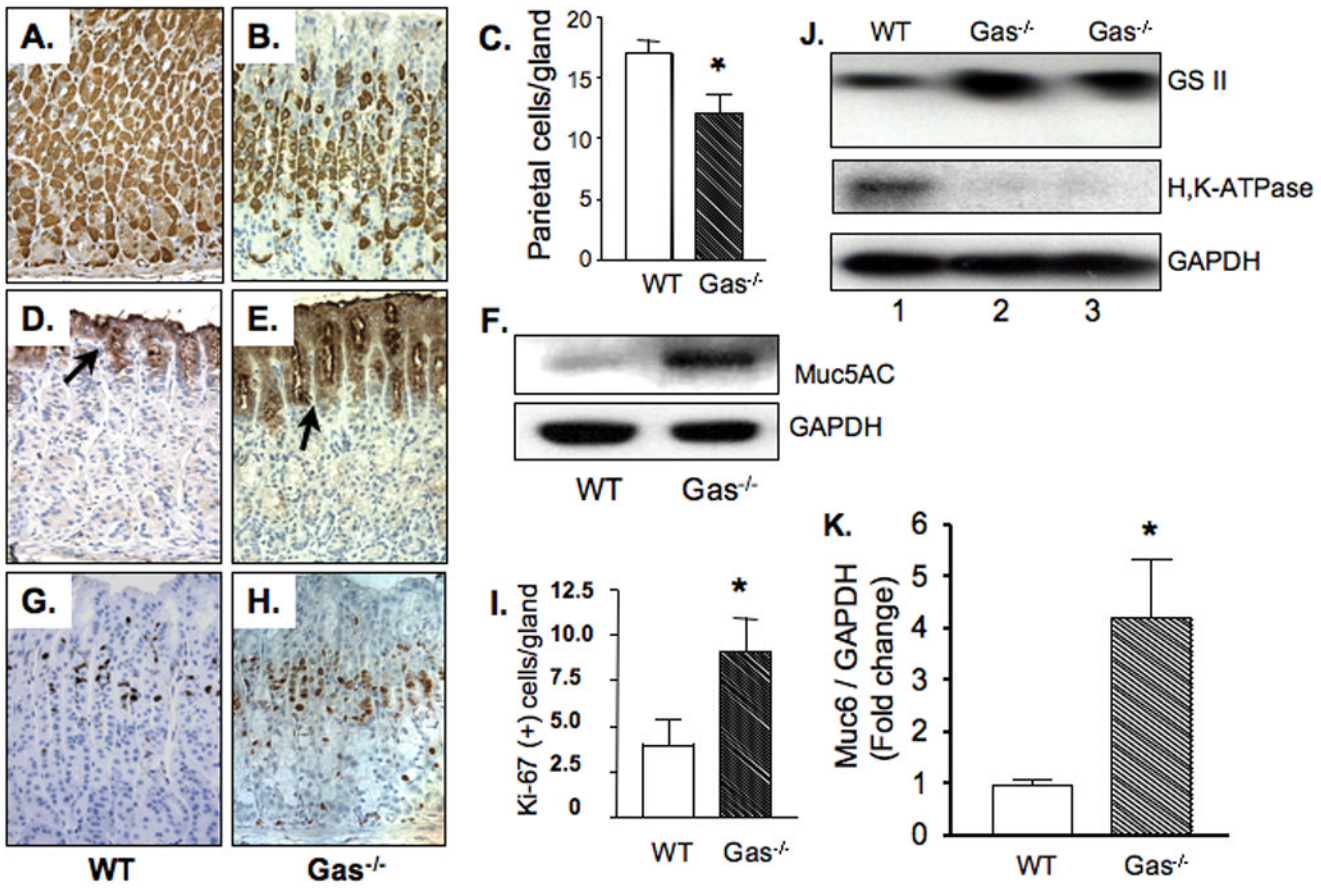

Figure 1. Corpus atrophy in 9 month Gas$^{-/-}$ mice

(A) Representative images of immunohistochemical staining of parietal cells with H^+,K^+-ATPase in 9 month WT (A) and Gas$^{-/-}$ mice (B) corpus. Positive cells were quantified by morphometry and expressed as the number of parietal cells/gland in Gas$^{-/-}$ mice (C). The surface pit cell population (arrows) were labeled using Muc5AC in 9 month WT (D) and Gas$^{-/-}$ mice (E). Immunoblotting was used to quantify the amount of Muc5AC protein in the WT and Gas$^{-/-}$ corpuses (F). Proliferating cells were stained for Ki67 in the WT (G) and Gas$^{-/-}$ (H) corpus mucosa and quantified by morphometry (I). N=9 for 9 month WT mice. N=12 for 9 month Gas$^{-/-}$ mice. *P<0.05 vs WT mice. Magnification, 400X. An increase in GSII mucin and a decrease in H^+K^+-ATPase protein are shown in a 9 month WT mouse and two 9 month Gas$^{-/-}$ mice (J). Muc6 mRNA was measured by qRT-PCR. N=9 for the WT group, N=12 for Gas$^{-/-}$ mice 9 month. *P<0.05 vs. WT mice (K).

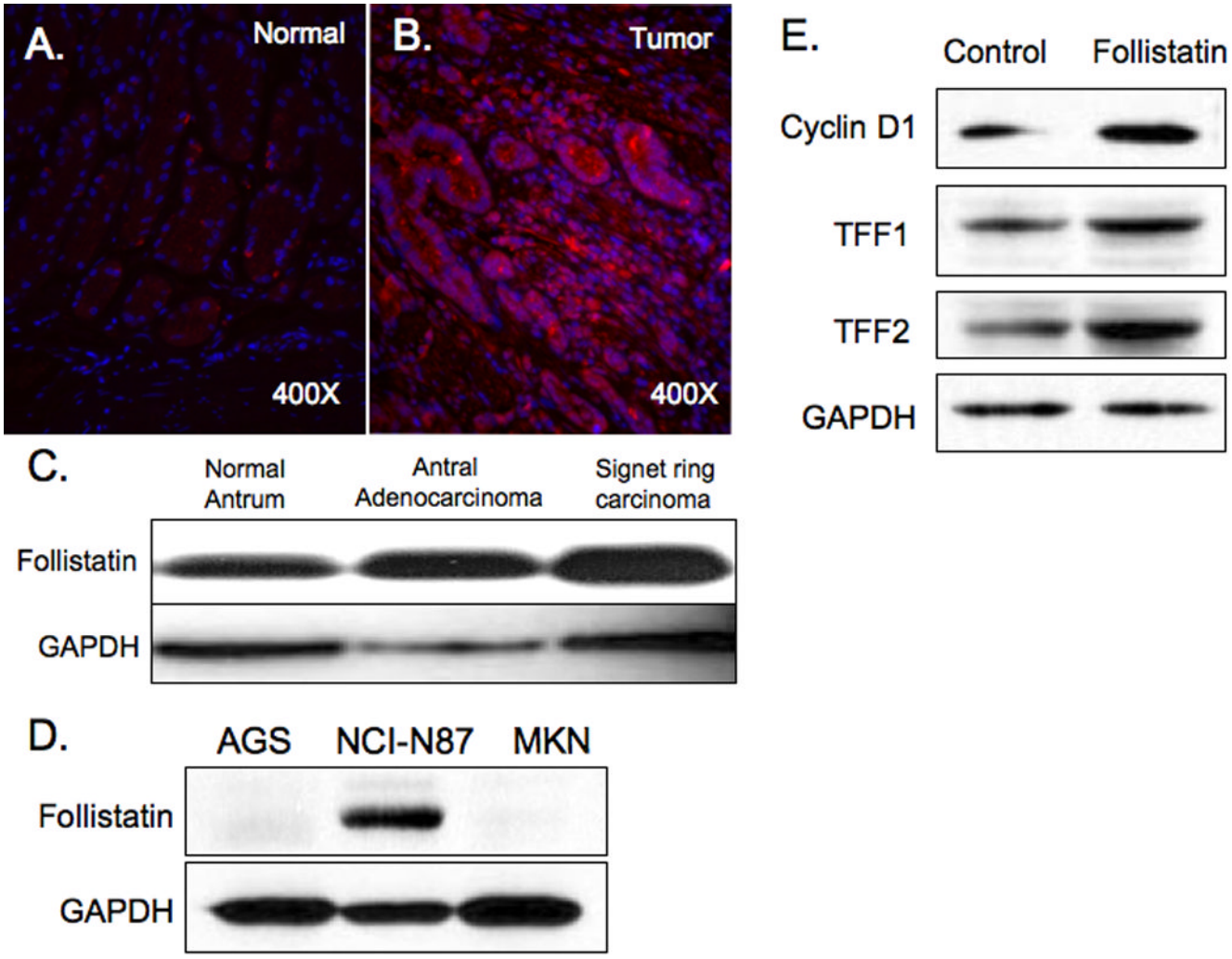

Figure 2. Follistatin expression elevated in human gastric cancer

Follistatin (red) expression in normal human antrum (A) and a tubular carcinoma (B) (magnification 400X) and by immunoblot in normal human antrum, antral adenocarcinoma and signet ring cell carcinoma (C). AGS, NCI-N87 and MKN45 gastric cancer cell line extracts immunoblotted for follistatin protein (D). NCI-N87 cells were treated with follistatin (0.5 μg/ml) for 24h then immunoblotted for cyclin D1, TFF1 and TFF2 (E). Control = untreated cells.

Table 1

Antral Changes in Gastrin-deficient mice

Up-regulated		Down-regulated
MMP 13 (59x)	Jagged1 (2.5x)	Angiogenin1 (−43x)
MMP 10 (17x)	Runx2 (2.5x)	H,K-ATPase (−29x)
IL 1R-like (13x)	Inhibin bA (2.5x)	Gastrin (−20x)
Mast cell protease (9x)	TNFrsf (2x)	Sfrp1 (−6x)
Ceacam1 (9x)	Sox 18 (2x)	GABAr (−5x)
Epiregulin (7x)	CyclinD2 (2x)	Necdin (−5x)
Vanin (7x)	EphRb2 (2x)	Msi2h (−4x)
IL 1β (7x)	HB-EGF (1.8x)	FGFbp 1 (−4x)
CXCl1 (7x)	Klf5 (1.6x)	TGFbR3 (−3x)
Follistatin (7x)	Nephronectin (4x)	Frzd 7 (−3x)
IGFbp3 (6x)	Claudin 4 & 23 (3x)	Barx1 (−2.5x)
Cathepsin E (6x)	Egr1 (3x)	Frzd 2 (−2.5x)
Clusterin (3x)	Sox 2 (3x)	Supervillin (−2x)
IL1rn (4x)	Amphiregulin (3x)	